Macromolecules

Article

pubs.acs.org/Macromolecules

Highly Thermally Stable, Transparent, and Flexible Polybenzoxazine Nanocomposites by Combination of Double-Decker-Shaped Polyhedral Silsesquioxanes and Polydimethylsiloxane

Yi-Ting Liao, Yung-Chih Lin, and Shiao-Wei Kuo*

Department of Materials and Optoelectronic Science, Center for Supramolecular Materials and Functional Polymers, National Sun Yat-Sen University, Kaohsiung, 804, Taiwan

Supporting Information

ABSTRACT: In this study a new type of bifunctional phenolic compound based on a double-decker silsesquioxane (DDSQ-BP) was synthesized from phenyltrimethylsilane and then reacted (Mannich condensation) with allylamine and CH_2O to form a bis-allyl benzoxazine DDSQ derivative (DDSQ-BZ). The structures of these DDSQ derivatives were confirmed using Fourier transform infrared and nuclear magnetic resonance spectroscopy and MALDI-TOF mass spectrometry. Highly thermally stable, transparent, and flexible polybenzoxazine prepolymers were obtained after hydrosilylation of DDSQ-BZ with polydimethylsiloxane (PDMS) as the flexible segment; these materials were characterized using differential scanning calorimetry, thermogravimetric analysis, microtensile testing, and UV−vis spectroscopy. The char yield of DDSQ-BZ-PDMS was 73 wt %, significantly higher than that of a typical polybenzoxazine; in addition, DDSQ-BZ-PDMS displayed high flexibility and transparency after thermal curing.

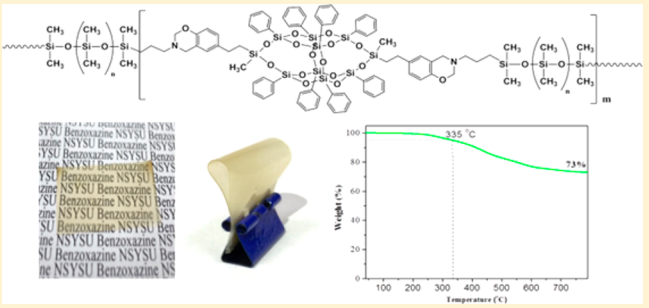

INTRODUCTION

The addition of polyhedral oligomeric silsesquioxane (POSS) derivatives into polymer matrices has received much interest recently because POSS nanoparticles (NPs) can enhance the thermal stability, decrease the flammability, lower the density, lower the thermal conductivity, increase the oxidation resistance, and lower the surface free energy.[1−8] In general, the architectures of polymer/POSS nanocomposites are dependent on the functionality presented by the POSS NPs.[9] In many cases, the POSS NPs are positioned at a chain end or side chain using a monofunctionalized POSS compound.[10−15] The addition of multifunctionalized POSS NPs into a polymer matrix usually results in insoluble cross-linked polymers; only a low content of POSS NPs is generally necessary when they present more than two functional units.[16−18] As a result, the incorporation of main-chain-type POSS units from bifunctionalized POSS NPs is an important procedure for developing new polymer/POSS nanocomposites,[19,20] especially for step-growth polymerization of polyimide (PI),[21,22] polyurethane (PU),[23] and polybenzoxazine (PBZ)[24] systems.

Benzoxazine monomers are new types of thermosetting resins (prepared through Mannich condensations of primary amines, phenolic derivatives, and CH_2O) that display physical properties superior to those of transitional epoxy or phenolic resins due to their strong intramolecular hydrogen bonding after thermal curing.[25−29] Another attractive feature of benzoxazine monomers is that they can undergo thermal curing without a catalyst to form polybenzoxazines that also have many excellent properties, including high thermal stability, low flammability, low dielectric constant, low surface free energy, and flexible molecular design.[30−33] A typical type of polybenzoxazine synthesized from bisphenol A, alanine, and CH_2O displays a glass transition temperature (T_g) of 180 °C.[25] Techniques to enhance the physical properties of such polybenzoxazines, by incorporating reactive functional units (e.g., carboxyl, allyl, propargyl, or thymine groups) into the benzoxazine monomers, have been examined widely.[34−36] In addition, blending of various inorganic compounds (e.g., clays, graphene, POSS, and carbon nanotubes) into benzoxazine monomers has also been adopted to form polybenzoxazine nanocomposites.[37−42] Nevertheless, these types of polybenzoxazines can still display brittleness and opacity after thermal curing.

The opacity and dark brown color of polybenzoxazines after thermal curing arises from carbonyl-containing units, namely 2,6-disubstituted benzoquinone units released from the isopropylidene linkages through cleavage and oxidation.[43] In this study, we prepared a bifunctional phenolic compound based on a double-decker silsesquioxane (DDSQ-BP) (Scheme 1a−e) to eliminate the possibility of forming a 2,6-disubstituted benzoquinone. Next, we prepared a bis-allyl benzoxazine DDSQ derivative (DDSQ-BZ) through Mannich condensation (Scheme 1f) and then formed, through hydrosilylation, a highly thermally stable, transparent, and flexible polybenzoxazine

Received: May 24, 2017
Revised: July 11, 2017
Published: July 20, 2017

DOI: 10.1021/acs.macromol.7b01085
Macromolecules 2017, 50, 5739−5747

Scheme 1. Preparation of the Prepolymer DDSQ-BZ-PDMS (g) from (a) Triphenylsilane, (b) DD-Na, (c) DDSQ, (d) DDSQ-BA, (e) DDSQ-BP, and (f) DDSQ-BZ

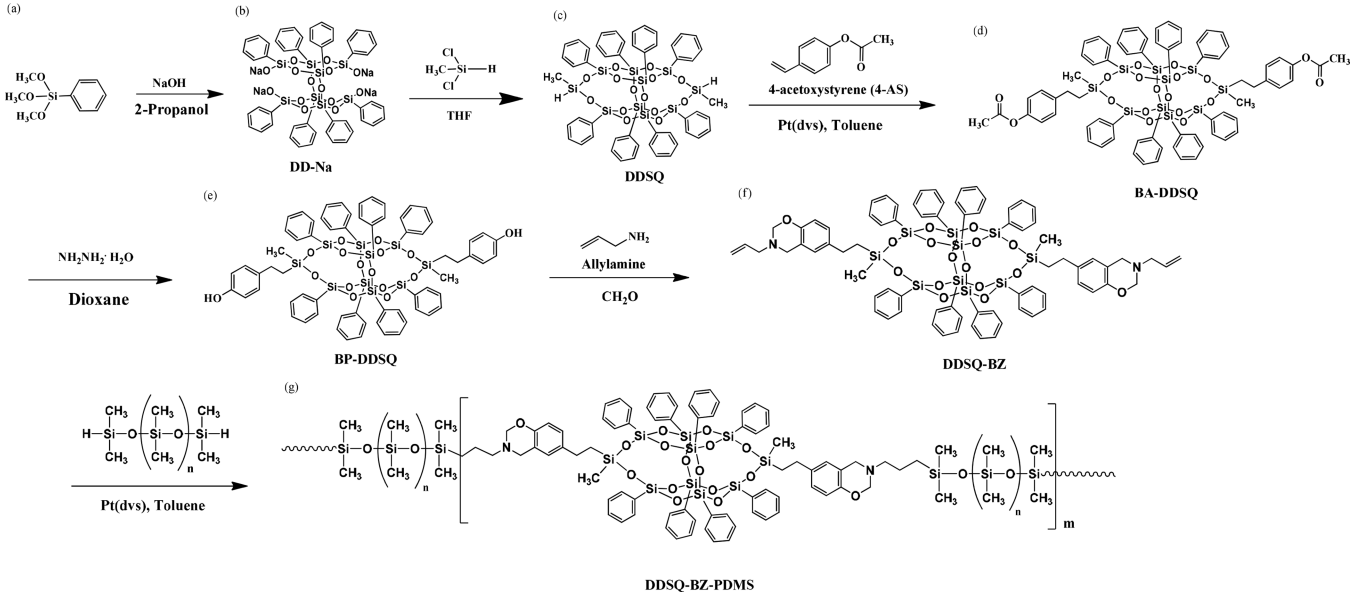

prepolymer incorporating polydimethylsiloxane (PDMS) as the flexible segment (Scheme 1g). Analyses using nuclear magnetic resonance (NMR) spectroscopy, matrix-assisted laser desorption ionization/time-of-flight mass spectrometry (MALDI-TOF MS), and Fourier transform infrared (FTIR) spectroscopy confirmed the chemical structures of these DDSQ derivatives. Differential scanning calorimetry (DSC), thermogravimetric analysis (TGA), scanning electron microscopy (SEM), microtensile testing, and FTIR and UV−vis spectroscopy were employed to investigate the thermal curing procedure and the thermal, mechanical, optical, and morphological properties of the polybenzoxazine/POSS nanocomposites.

EXPERIMENTAL SECTION

Materials. Phenyltrimethylsilane, methyldichlorosilane, platinum divinyltetramethyldisiloxane complex [Pt(dvs)], sodium hydroxide (NaOH), 2-propanol, hydrazine monohydrate, charcoal, tetrahydrofuran (THF), and magnesium sulfate ($MgSO_4$) were purchased from Alfa-Aesar. Ethyl acetate, sodium bicarbonate ($NaHCO_3$), methanol (MeOH), ethanol (EtOH), *n*-hexane, xylene, 1,4-dioxane, paraformaldehyde, 4-acetoxystyrene, allylamine, and hydride-terminated polydimethylsiloxane (PDMS; M_n = 580 g/mol) were purchased from Sigma-Aldrich.

Double-Decker Silsesquioxane-Na (DD-Na). NaOH (14 g) and 2-propanol (300 mL) were placed in a three-neck flask equipped with a reflux condenser. Deionized H_2O (10 mL) and phenyltrimethylsilane (105 g) were added, and then the blend was mixed thoroughly and heated under reflux for 24 h. The oil bath was removed, and then the mixture was stirred for 8 h at room temperature until the reaction was complete. Alternatively, the oil bath was removed after reflux for 12 h, and then the mixture was stirred for 48 h at room temperature. The solvent was evaporated through vacuum distillation, and the residue was dried in a vacuum oven to obtain a white powder.

Double-Decker Silsesquioxane. DD-Na (11.6 g, 10.0 mmol) was placed in a three-neck flask equipped with a reflux condenser, and then triethylamine (4.00 g, 40.0 mmol) and THF (200 mL) were added. The three-neck flask was cooled in an ice bath, and the mixture was stirred thoroughly. Methyldichlorosilane (4.50 g, 40.0 mmol) was added as an end-capping reactant into the flask, and then the mixture was left for 6 h at room temperature. The filtrate was washed with deionized water and saturated $NaHCO_3$. The organic phase was dried ($MgSO_4$) and concentrated. The solid residue was washed several times with MeOH and MeCN and then dried (vacuum oven) to obtain a white powder. MALDI-TOF mass analyses: 1176.16 g mol^{-1} for $[DDSQ + Na]^+$: calcd: 1176.76 g mol^{-1}.

Bis-Phenyl Acetate Double-Decker Silsesquioxane (DDSQ-BA). DDSQ (10.0 g, 8.68 mmol), 4-acetoxystyrene (8.60 g, 52.1 mmol), and toluene (100 mL) were placed in a three-neck flask equipped with a reflux condenser and stirred thoroughly until transparent. After heating under reflux under N_2, 0.03 wt % of platinum (Pt(dvs)) was added as the catalyst. The oil bath was removed after the reaction was complete. The mixture was filtered, and the filtrate was concentrated through vacuum distillation to obtain a solid, which was dried in a vacuum oven to obtain a milky product. MALDI-TOF mass analyses: 1500.30 g mol^{-1} for $[DDSQ\text{-}BA + Na]^+$: calcd: 1501.13 g mol^{-1}.

Bis-Phenolic Double-Decker Silsesquioxane (DDSQ-BP). DDSQ-BA (10.0 g, 6.78 mmol) and dioxane (100 mL) were placed into three-neck flask equipped with a reflux condenser and stirred thoroughly until dissolution occurred. Hydrazine monohydrate (3.39 g, 67.8 mmol) was added. When the reaction was complete, the mixture was precipitated in deionized H_2O and extracted with EtOAc. Concentration of the organic phase through vacuum distillation gave a solid, which was dried under vacuum to give milky powder. MALDI-TOF mass analyses: 1415.88 g mol^{-1} for $[DDSQ\text{-}BA + Na]^+$: calcd: 1417.06 g mol^{-1}.

Bis-Allyl Benzoxazine Double-Decker Silsesquioxane (DDSQ-BZ). DDSQ-BP (20.0 g, 14.4 mmol), CH_2O (3.48 g, 115 mmol), and *p*-xylene (200 mL) were placed in a three-neck flask equipped with a reflux condenser. After N_2 gas replacement (three times), allylamine (3.28 g, 57.4 mmol) was added under N_2. The mixture was heated at 90 °C for 48 h. The oil bath was removed after the reaction was complete, and the mixture was subjected to gravity filtration. The solvent was evaporated using a rotary evaporator, and the residue was dried in a vacuum oven to give a yellow powder. MALDI-TOF mass analyses: 1579.30 g mol^{-1} for $[DDSQ\text{-}BA + Na]^+$: calcd: 1579.29 g mol^{-1}.

Polydimethylsiloxane-Benzoxazine Double-Decker Silsesquioxane (DDSQ-BZ-PDMS) Prepolymer. DDSQ-BZ (10.0 g, 6.43 mmol) and PDMS (3.70 g, 6.43 mmol) were dissolved in toluene (200 mL) in a three-neck flask equipped with a reflux condenser. The mixture was stirred thoroughly and heated at 70 °C under reflux under N_2, and then 0.03 wt % of platinum (Pt(dvs)) was added. The oil bath was removed after the reaction had reached completion. The mixture was filtered, and then the filtrate was concentrated through vacuum

DOI: 10.1021/acs.macromol.7b01085
Macromolecules 2017, 50, 5739−5747

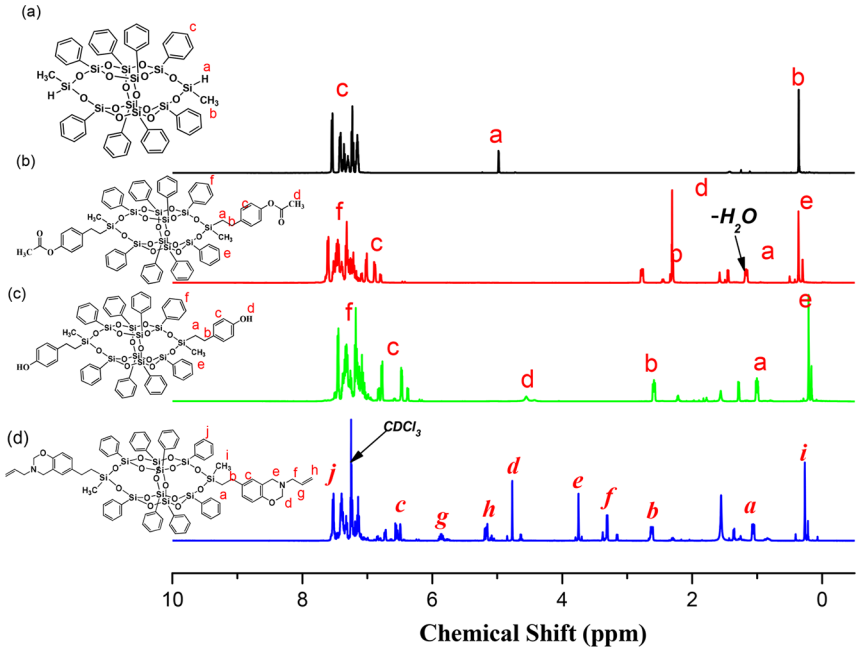

Figure 1. ^{1}H NMR spectra of (a) DDSQ, (b) DDSQ-BA, (c) DDSQ-BP, and (d) DDSQ-BZ.

distillation to obtain a solid, which was dried in a vacuum oven to give the DDSQ-BZ-PDMS prepolymer (M_n = 7300 g/mol; PDI = 1.77).

Thermal Curing of DDSQ-BZ and DDSQ-BZ-PDMS. Desired amounts of DDSQ-BZ or DDSQ-BZ-PDMS were placed in an aluminum pan and then subjected to thermal curing at 100, 140, 180, 200, 220, and 240 °C for 2 h. The DDSQ-BZ sample formed a red color that darkened as the thermal curing temperature increased. In contrast, the DDSQ-BZ-DDSQ sample formed a transparent film after thermal curing.

Characterization. ^{1}H and ^{13}C NMR spectra were recorded using an INOVA 500 spectrometer, with $CDCl_3$ or DMSO-d_6 as the solvent and the tetramethylsilane (TMS) as the external standard. A Bruker Tensor 27 FTIR spectrophotometer and the conventional KBr disk method. The sample should be thin to obey the Beer−Lambert law and then were used to record FTIR spectra, with 32 scans collected at a spectral resolution of 4 cm^{-1}; a temperature-controlled compartment holder was used to record FTIR spectra at various temperatures under the N_2 atmosphere to remain the sample film drying. Mass spectra of the DDSQ derivatives were recorded using a Bruker Daltonics Autoflex MALDI-TOF mass spectrometer. Molecular weights were determined using a Bruker Solarix high-resolution Fourier transform mass spectrometry system. Dynamic thermal curing kinetics were measured using a TA Q-20 differential scanning calorimeter with ca. 7 mg sample on the DSC sample pan under a N_2 atmosphere (100 mL min^{-1}), with heating from 30 to 350 °C at a heating rate of 20 °C min^{-1}. The thermal decomposition temperatures and char yields of all the DDSQ derivatives were determined using a TA Q-50 thermogravimetric analyzer operated under a N_2 atmosphere (60 mL min^{-1}), with heating from 30 to 800 °C at a heating rate of 20 °C min^{-1}. The mechanical properties of DDSQ-BZ and DDSQ-BZ-PDMS were characterized using an MTS tytron 250 microtensile testing machine. The tested films had dimensions of approximately 10 mm × 10 mm × 0.1 mm; the tensile rates were tested at 0.015 mm s^{-1}, using a load cell to mediate the tensile force. UV−Vis spectra of cured thin films of DDSQ-BZ and DDSQ-BZ-PDMS were recorded using a Shimadzu mini 1240 spectrophotometer. SEM images of the cured DDSQ-BZ-PDMS sample and poly(BA-a)/PDMS blend sample were recorded using a JEOL JSM-6700F microscope operated at 30 kV.

RESULTS AND DISCUSSION

Synthesis of Bis-Allyl Benzoxazine Double-Decker Silsesquioxane (DDSQ-BZ). Scheme 1 presents our synthesis

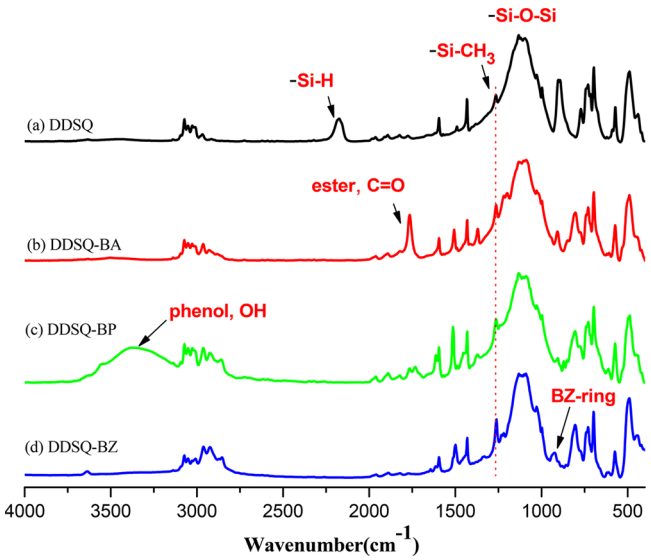

Figure 2. FTIR spectra of (a) DDSQ, (b) DDSQ-BA, (c) DDSQ-BP, and (d) DDSQ-BZ.

of the double-decker silsesquioxane (DDSQ) from phenyltrimethylsilane. The DDSQ derivatives prepared in this study were all characterized using NMR and FTIR spectroscopy and MALDI-TOF mass spectrometry. Figure 1 presents ^{1}H NMR spectra of the DDSQ derivatives and also summarizes the peak assignments. The spectrum of DDSQ (Figure 1a) features signals for the Si−**H** protons at 4.98 ppm, Si−C**H**$_3$ protons at 0.36 ppm, and aromatic protons at 7.14−7.50 ppm. The spectrum of DDSQ-BA (Figure 1b) reveals that the signal of the Si−**H** protons (4.98 ppm) has disappeared, while a signal for the acetyl groups (O═C−C**H**$_3$) is now present at 2.29 ppm, with the signal for the Si−C**H**$_3$ protons remaining at 0.36 ppm, indicative of complete hydrosilylation. The signal of the acetyl group (O═C−C**H**$_3$) at 2.29 ppm disappeared after hydrolysis (Figure 1c), with a broad peak for the phenolic protons now located at 4.56 ppm, confirming the synthesis of

DOI: 10.1021/acs.macromol.7b01085
Macromolecules 2017, 50, 5739−5747

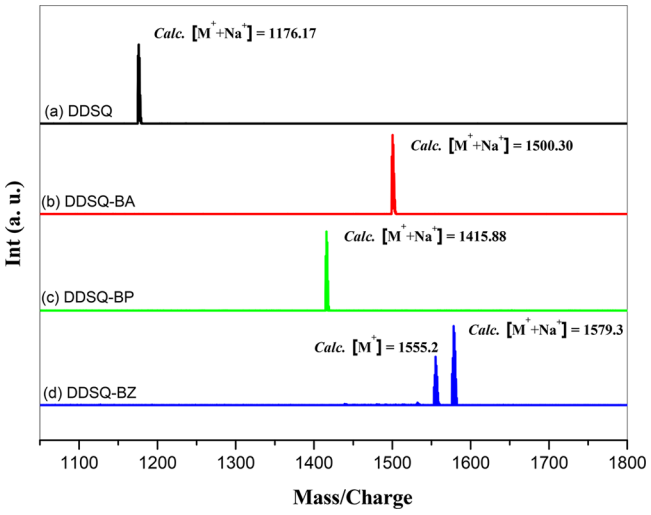

Figure 3. MALDI-TOF mass spectra of (a) DDSQ, (b) DDSQ-BA, (c) DDSQ-BP, and (d) DDSQ-BZ.

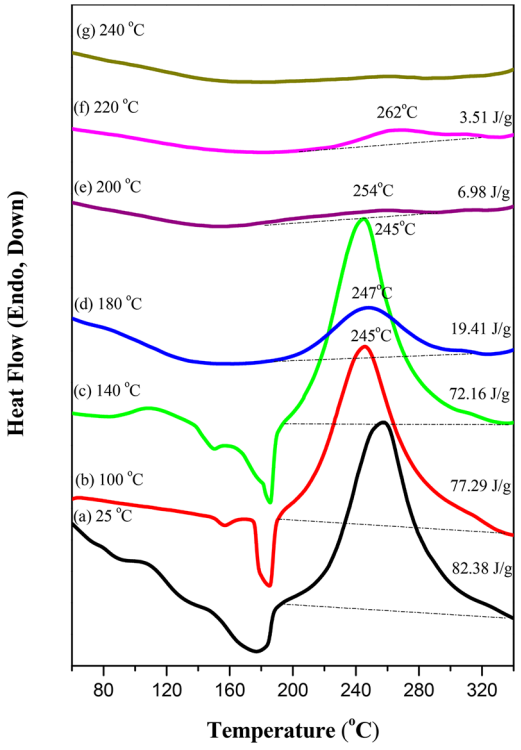

Figure 4. DSC traces of uncured DDSQ-BZ, recorded after each curing stage.

DDSQ-BP. The signal for the phenolic protons was absent, and signals appeared for the methylene bridge protons of the benzoxazine ring at 3.74 and 4.78 ppm in the spectrum of DDSQ-BZ (Figure 1d). Signals for vinyl protons appeared at 5.87 and 5.16 ppm in a 1:2 ratio, while a signal for the protons between the vinyl unit and the nitrogen atom was located at 3.30 ppm (peak f), confirming the synthesis of DDSQ-BZ.

Similar conclusions were drawn from the corresponding ^{13}C NMR spectra (Figure S1), the peaks of which are summarized in Scheme S1. For pure DDSQ, the signal of the Si−CH_3 carbon nuclei appeared at 0.58 ppm, while those for the aromatic ring carbon nuclei were located at 128.50−134.67 ppm (Figure S1a). After hydrosilylation to give DDSQ-BA,

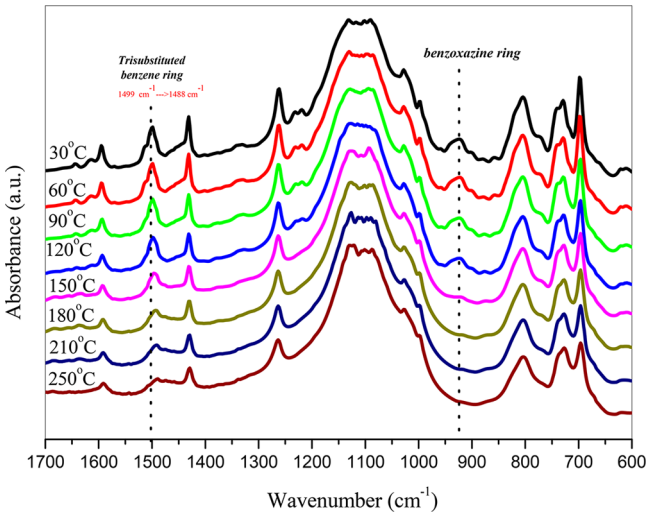

Figure 5. FTIR spectra of uncured DDSQ-BZ, recorded after each curing stage.

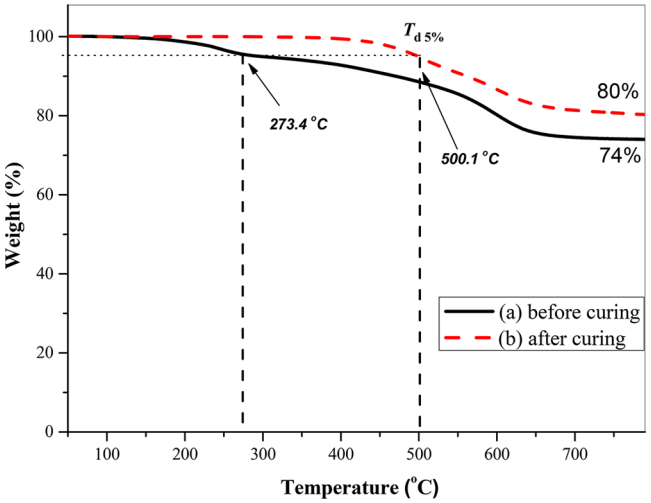

Figure 6. TGA analyses of (a) uncured and (b) thermally cured DDSQ-BZ.

signals for the acetyl groups appeared at 170.39 (C═O) and 18.66 (CH_3) ppm and for the methylene units at 21.11 and 28.52 ppm (Figure S1b). The signal of the C═O carbon nuclei of the acetyl groups at 170.39 ppm disappeared after hydrolysis, with the signal of the phenolic carbon atom (peak f in Scheme S1c) (at 149.12 ppm for DDSQ-BA) shifting significantly downfield to 153.57 ppm (Figure S1c), confirming the synthesis of DDSQ-BP. Characteristic signals for the OCH_2N and ArCH_2N units of the benzoxazine rings appeared at 82.39 and 54.50 ppm, respectively, in Figure S1d, with a signal for the carbon atoms between the vinyl units and nitrogen atoms located at 49.87 ppm (peak g in Scheme S1d), confirming the synthesis of DDSQ-BZ.

Figure 2 summarizes the FTIR spectra of DDSQ, DDSQ-BA, DDSQ-BP, and DDSQ-BZ. A strong absorption signal near 1087 cm^{-1}, representing siloxane units (Si−O−Si), was a general feature in the spectrum of each DDSQ derivative. The Si−H stretching vibration of DDSQ appeared at 2172 cm^{-1} (Figure 2a); it was absent for DDSQ-BA (Figure 2b), suggesting complete hydrosilylation, while a signal for the C═O units of the acetoxystyrene groups was present at 1765

DOI: 10.1021/acs.macromol.7b01085
Macromolecules 2017, 50, 5739−5747

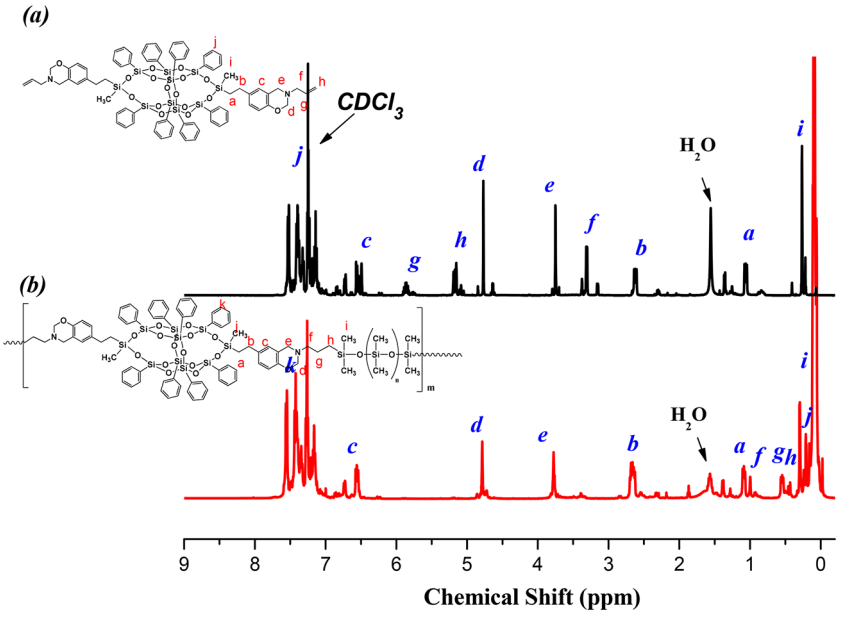

Figure 7. ^{1}H NMR spectra of (a) DDSQ-BZ and (b) DDSQ-BZ-PDMS.

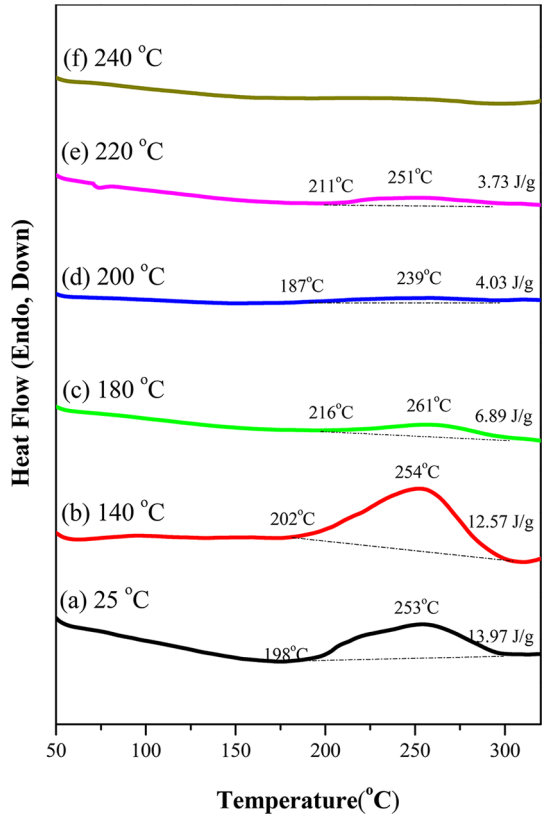

Figure 8. DSC traces of uncured DDSQ-BZ-PDMS, recorded after each curing stage.

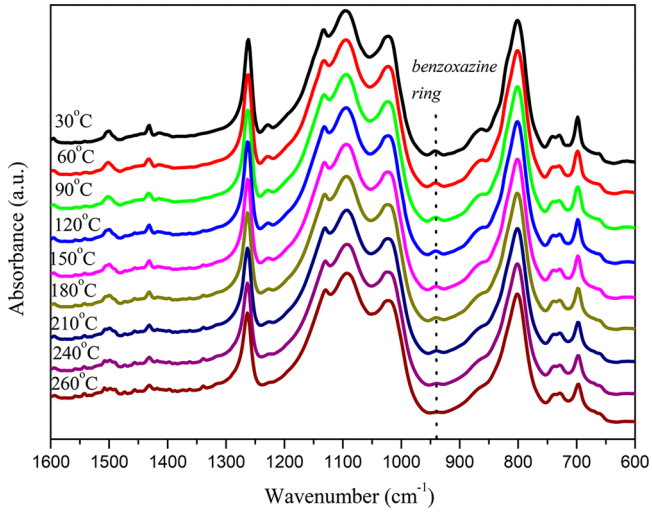

Figure 9. FTIR spectra of uncured DDSQ-BZ-PDMS, recorded after each curing stage.

cm^{-1}. After hydrolysis to give DDSQ-BP (Figure 2c), the C═O absorption disappeared and a broad peak appeared at 3382 cm^{-1} representing the phenolic OH groups. The signal for the OH groups was absent from the spectrum of DDSQ-BZ (Figure 2d), with a peak at 921 cm^{-1} (corresponding to the out-of-plane C−H vibration of the benzoxazine ring) confirming its synthesis.

Figure 3 presents MALDI-TOF mass spectra of the DDSQ derivatives, with monodisperse mass distributions at 1176 g mol^{-1} for [DDSQ + Na]$^{+}$, 1500 g mol^{-1} for [DDSQ-BA + Na]$^{+}$, and 1415 g mol^{-1} for [DDSQ-BP + Na]$^{+}$ and two mass distributions at 1555 g mol^{-1} for [DDSQ-BZ]$^{+}$ and 1579 g mol^{-1} for [DDSQ-BZ + Na]$^{+}$. Good correlations existed between the calculated and experimental molecular masses, implying well-defined structures for all of the DDSQ derivatives. Taking into consideration all of the data from the NMR, FTIR, and MALDI-TOF mass spectra, we could confirm the successful synthesis of DDSQ-BZ.

Thermal Properties of DDSQ-BZ. We performed DSC analyses (Figure 4) to observe the sample that was heated to polymerize of DDSQ-BZ. The melting temperature near 180 °C for the uncured DDSQ-BZ suggested that it had reasonable purity. A thermal curing exotherm was observed at 258 °C with a reaction heat of 82.38 J g^{-1} (Figure 4a). The reaction heat decreased upon increasing the thermal curing temperature; the

DOI: 10.1021/acs.macromol.7b01085
Macromolecules 2017, 50, 5739−5747

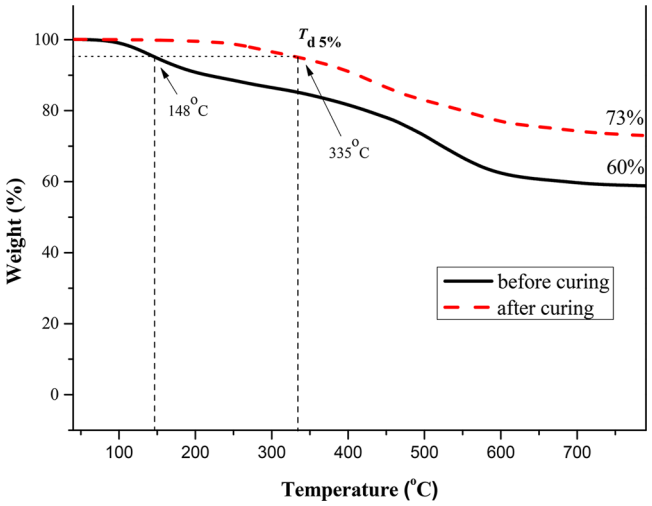

Figure 10. TGA analyses of uncured and thermally cured DDSQ-BZ-PDMS.

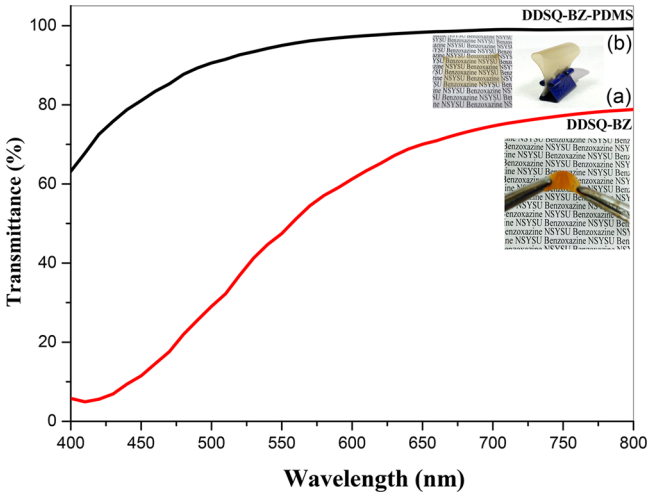

Figure 11. UV spectra of thermally cured DDSQ-BZ (thickness: 0.15 mm) and DDSQ-BZ-PDMS (thickness: 0.12 mm).

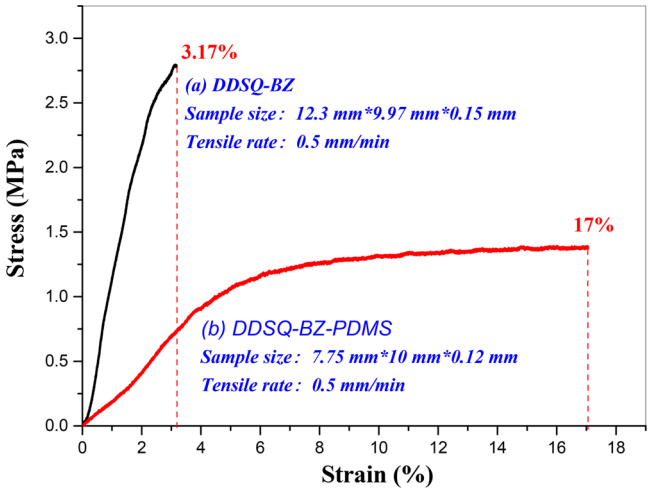

Figure 12. Stress/strain curves of thermally cured DDSQ-BZ and DDSQ-BZ-PDMS.

thermal curing exotherm peak almost disappeared completely after thermal curing at a temperature of 240 °C (Figure 4g). FTIR spectra confirmed this phenomenon after the thermal curing of DDSQ-BZ. The main characteristic absorption peaks for uncured DDSQ-BZ appeared at 921 cm^{-1} (benzoxazine ring), 1499 cm^{-1} (trisubstituted aromatic ring), and 1644 cm^{-1} (stretching of C=C bonds); the intensities of those signals gradually decreased upon increasing the thermal curing temperature, almost disappearing completely after thermal curing at 240 °C (Figure 5). The peaks at 1087 and 1263 cm^{-1}, corresponding to the Si−O−Si and Si−CH_3 vibrations, remained, implying that the DDSQ cage structure did not break during the thermal curing of DDSQ-BZ.[21−23]

Figure 6 displays the TGA traces of DDSQ-BZ before and after thermal curing under a N_2 atmosphere. For the uncured DDSQ-BZ, the thermal decomposition temperature at 5 wt % loss (T_{d5}) was 273.4 °C, and the char yield was 74 wt %; the thermal decomposition temperature increased significantly to 500.1 °C for the thermally cured DDSQ-BZ, with the char yield also increasing to 80 wt %. To the best of our knowledge,[25] our thermally cured DDSQ-BZ has thermal stability superior to that of any other reported polybenzoxazine resin, presumably because of its combination of allyl groups (increased cross-linking density)[44] and DDSQ cage structures (increased thermal resistance).[23,24]

Synthesis of DDSQ-BZ-PDMS. DDSQ-BZ underwent further hydrosilylation with hydride-terminated PDMS to form DDSQ-BZ-PDMS (Scheme 1). Figure 7 presents ^1H NMR spectra of DDSQ-BZ and DDSQ-BZ-PDMS. The signals for the vinyl protons of DDSQ-BZ at 5.87 and 5.16 ppm were absent in the spectrum of DDSQ-BZ-PDMS, while the signals for the protons between the vinyl units and nitrogen atoms (peak f) shifted from 3.30 to 1.00 ppm. The most important characteristic signals at 3.74 and 4.78 ppm, corresponding to the methylene bridge protons of the benzoxazine ring, remained, confirming the synthesis of DDSQ-BZ-PDMS. A similar conclusion could be drawn from the ^{13}C NMR spectra of DDSQ-BZ and DDSQ-BZ-PDMS (Figure S2), where the signals for the vinyl carbon atoms disappeared and those for aliphatic carbon atoms appeared at relatively high field, while the characteristic signals for the benzoxazine ring remained at 82.39 and 54.50 ppm, indicative of the synthesis of DDSQ-BZ-PDMS. Because DDSQ-BZ-PDMS was a prepolymer after the hydrosilylation, we used GPC analysis to measure its molecular weight (ca. 7000 g mol^{-1}).

Thermal and Mechanical Properties of DDSQ-BZ-PDMS. We performed DSC analyses (Figure 8) to investigate the sample that was heated to polymerize of DDSQ-BZ-PDMS. Similar to the DSC traces of DDSQ-BZ, Figure 8a reveals that DDSQ-BZ-PDMS also displayed an exotherm peak centered at 253 °C with a reaction heat of 13.97 J g^{-1}. Because the fraction of benzoxazine rings in DDSQ-BZ-PDMS was smaller relative to that in DDSQ-BZ, it is reasonable that the reaction heat was also smaller. The reaction heat decreased upon increasing the thermal curing temperature, with the thermal curing exotherm peak almost disappearing completely after thermal curing at 240 °C (Figure 8f). Similar behavior was evident in the FTIR spectra recorded after thermal curing of DDSQ-BZ-PDMS (Figure 9). The main characteristic absorption peak for uncured DDSQ-BZ appeared at 942 cm^{-1} (benzoxazine ring); its intensity decreased gradually upon increasing the thermal curing temperature, almost disappearing completely after thermal curing at 240 °C. The peaks at 1093 and 1261 cm^{-1}, representing Si−O−Si and Si−CH_3 vibrations, remained,

DOI: 10.1021/acs.macromol.7b01085
Macromolecules 2017, 50, 5739−5747

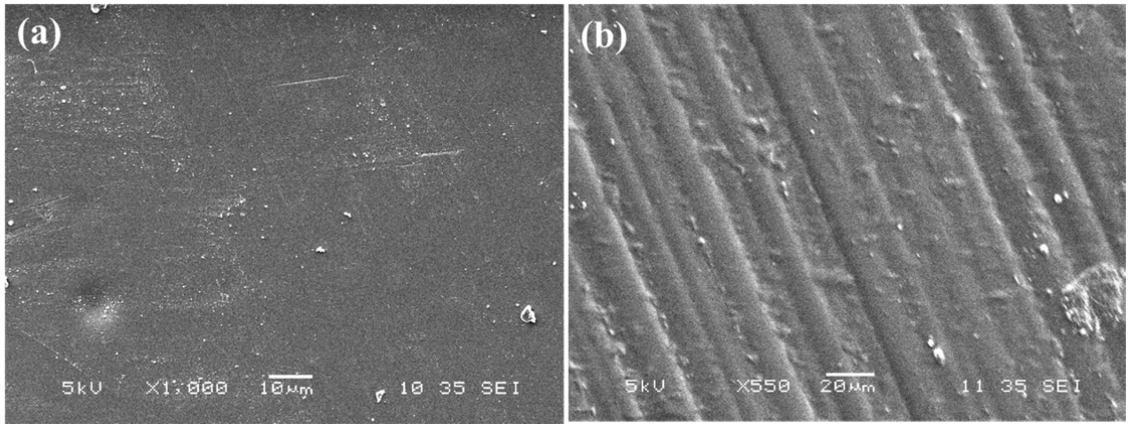

Figure 13. SEM images of thermally cured (a) DDSQ-BZ and (b) DDSQ-BZ-PDMS.

implying that the DDSQ cage structure did not destruct after thermal curing of DDSQ-BZ-PDMS.

Figure 10 displays TGA traces of DDSQ-BZ-PDMS before and after its thermal curing under N_2. For the uncured DDSQ-BZ-PDMS, the thermal decomposition temperature was 148 °C, and the char yield was 60 wt %; the thermal decomposition temperature also underwent a significant increase to 335 °C after thermal curing of DDSQ-BZ-PDMS, with the char yield also increasing to 73 wt %. Compared with the DDSQ-BZ after thermal curing, the thermally cured DDSQ-BZ-PDMS had a relatively lower thermal decomposition temperature and char yield because of the flexible PDMS segment and a lack of vinyl-terminated groups (therefore, a lower cross-linking density).

We found, however, that the transparency of DDSQ-BZ-PDMS was better than that of DDSQ-BZ after thermal curing (Figure 11). The thermally cured DDSQ-BZ-PDMS displayed higher transparency, no brown color, and better flexibility (Figure 11b) than the thermally cured DDSQ-BZ (Figure 11a). In addition, the elongation of the thermally cured DDSQ-BZ-PDMS was better than that of the thermally cured DDSQ-BZ (Figure 12). Thus, the incorporation of flexible PDMS segments into the DDSQ-BZ matrix enhanced both the transparency and flexibility.

Although the thermal stability decreased slightly after the incorporation of the PDMS segments, we note that conventional 3-phenyl-3,4-dihydro-2*H*-benzooxazine (P-a type of benzoxazine) provides a thermal decomposition temperature of approximately 320 °C and a char yield of 40 wt %.[25] Thus, the thermally cured DDSQ-BZ-PDMS possesses not only improved thermal stability (T_d = 335 °C; char yield = 70 wt %) but also higher transparency and flexibility relative to this P-a type polybenzoxazine.

Figure 13 displays SEM images of DDSQ-BZ and DDSQ-BZ-PDMS after thermal curing, revealing smooth surfaces and no macrophase separation of the DDSQ and PDMS segments. For comparison, Figure S3 provides SEM images recorded after thermal curing of bisphenol/aniline benzoxazine monomer (BA-a type) blended with PDMS segments at 7 and 13 wt %. The pure BA-a type polybenzoxazine also featured a smooth surface with no macrophase separation, but blending with 7 and 13 wt % of PDMS (Figures S3b and S3c, respectively) resulted in macrophase separation (ca. 2−3 μm) in this thermoset/thermoplastic blend system. Thus, the combination of the rigid DDSQ cage structure and the flexible PDMS segments in the benzoxazine matrix of DDSQ-BZ-PDMS, linked through covalent bonds, improved the thermal and mechanical properties, ensured high transparency and flexibility, and inhibited macrophase separation of the DDSQ cage structures and PDMS segments.

CONCLUSIONS

We have synthesized highly thermally stable, transparent, and flexible polybenzoxazine nanocomposites incorporating DDSQ and PDMS units, with their structures, and those of the synthetic intermediates, confirmed using NMR and FTIR spectroscopy and MALDI-TOF mass spectrometry. The thermal decomposition temperature of DDSQ-BZ after thermal curing was 500 °C, and the char yield was 80 wt %; we believe that this polybenzoxazine resin has the highest thermal stability ever reported. After hydrosilylation with PDMS to form DDSQ-BZ-PDMS, thermal curing provided a transparent and flexible polybenzoxazine exhibiting high thermal stability. As a result, this approach overcomes two of the major drawbacks of polybenzoxazines: their brittleness and opacity.

ASSOCIATED CONTENT

Supporting Information

The Supporting Information is available free of charge on the ACS Publications website at DOI: 10.1021/acs.macromol.7b01085.

Peak assignments for ^{13}C NMR spectra and SEM images (Figures S1−S3) (PDF)

AUTHOR INFORMATION

Corresponding Author

*E-mail: kuosw@faculty.nsysu.edu.tw (S.-W.K.).

ORCID

Shiao-Wei Kuo: 0000-0002-4306-7171

Notes

The authors declare no competing financial interest.

ACKNOWLEDGMENTS

This study was supported financially by the Ministry of Science and Technology, Taiwan, under contracts MOST103-2221-E-110-079-MY3 and MOST105-2221-E-110-092-MY3.

REFERENCES

(1) Zhang, W.; Camino, G.; Yang, R. Polymer/polyhedral oligomeric silsesquioxane (POSS) nanocomposites: An overview of fire retardance. *Prog. Polym. Sci.* **2017**, *67*, 77−125.

DOI: 10.1021/acs.macromol.7b01085
Macromolecules 2017, 50, 5739−5747

(2) Zhang, W.; Muller, A. H. E. Architecture, self-assembly and properties of well-defined hybrid polymers based on polyhedral oligomeric silsequioxane (POSS). *Prog. Polym. Sci.* **2013**, *38*, 1121−1162.
(3) Franczyk, A.; He, H.; Burdynska, J.; Hui, C. M.; Matyjaszewski, K.; Marciniec, B. Synthesis of High Molecular Weight Polymethacrylates with Polyhedral Oligomeric Silsesquioxane Moieties by Atom Transfer Radical Polymerization. *ACS Macro Lett.* **2014**, *3*, 799−802.
(4) Li, Z.; Wu, D.; Liang, Y.; Fu, R.; Matyjaszewski, K. Synthesis of Well-Defined Microporous Carbons by Molecular-Scale Templating with Polyhedral Oligomeric Silsesquioxane Moieties. *J. Am. Chem. Soc.* **2014**, *136*, 4805−4808.
(5) Tong, C.; Tian, Z.; Chen, C.; Li, Z.; Modzelewski, T.; Allcock, H. Synthesis and Characterization of Trifluoroethoxy Polyphosphazenes Containing Polyhedral Oligomeric Silsesquioxane (POSS) Side Groups. *Macromolecules* **2016**, *49*, 1313−1320.
(6) Chiou, C. W.; Lin, Y. C.; Wang, L.; Maeda, R.; Hayakawa, H.; Kuo, S. W. Hydrogen Bond Interactions Mediate Hierarchical Self-Assembly of POSS-Containing Block Copolymers Blended with Phenolic Resin. *Macromolecules* **2014**, *47*, 8709−8721.
(7) Hu, W. H.; Huang, K. W.; Chiou, C. W.; Kuo, S. W. Complementary Multiple Hydrogen Bonding Interactions Induce the Self-Assembly of Supramolecular Structures from Heteronucleobase-Functionalized Benzoxazine and Polyhedral Oligomeric Silsesquioxane Nanoparticles. *Macromolecules* **2012**, *45*, 9020−9028.
(8) Mohamed, M. G.; Hsu, K. C.; Hong, J. L.; Kuo, S. W. Unexpected fluorescence from maleimide-containing polyhedral oligomeric silsesquioxanes: nanoparticle and sequence distribution analyses of polystyrene-based alternating copolymers. *Polym. Chem.* **2016**, *7*, 135−145.
(9) Kuo, S. W.; Chang, F. C. POSS related polymer nanocomposites. *Prog. Polym. Sci.* **2011**, *36*, 1649−1696.
(10) Leu, C. M.; Chang, Y. T.; Wei, H. W. Synthesis and Dielectric Properties of Polyimide-Tethered Polyhedral Oligomeric Silsesquioxane (POSS) Nanocomposites via POSS-diamine. *Macromolecules* **2003**, *36*, 9122−9127.
(11) Lin, Y. C.; Kuo, S. W. Self-assembly and secondary structures of linear polypeptides tethered to polyhedral oligomeric silsesquioxane nanoparticles through click chemistry. *J. Polym. Sci., Part A: Polym. Chem.* **2011**, *49*, 2127−2137.
(12) Huang, M.; Hsu, C. H.; Wang, J.; Mei, S.; Dong, X.; Li, Y.; Li, M.; Liu, H.; Zhang, W.; Aida, T.; Zhang, W. B.; Yue, K.; Cheng, S. Z. D. Selective assemblies of giant tetrahedra via precisely controlled positional interactions. *Science* **2015**, *348*, 424−428.
(13) Liu, H.; Luo, J.; Shan, W.; Guo, D.; Wang, J.; Hsu, C. H.; Huang, M.; Zhang, W.; Lotz, B.; Zhang, W. B.; Yue, K.; Liu, T.; Cheng, S. Z. D. Toward Controlled Hierarchical Heterogeneities in Giant Molecules with Precisely Arranged Nano Building Blocks. *ACS Nano* **2016**, *10*, 6585−6596.
(14) Xu, H.; Kuo, S. W.; Lee, J. S.; Chang, F. C. Preparations, Thermal Properties, and Tg Increase Mechanism of Inorganic/Organic Hybrid Polymers Based on Polyhedral Oligomeric Silsesquioxanes. *Macromolecules* **2002**, *35*, 8788−8793.
(15) Huang, C. F.; Kuo, S. W.; Lin, F. J.; Huang, W. J.; Wang, C. F.; Chen, W. Y.; Chang, F. C. Influence of PMMA-chain-end tethered polyhedral oligomeric silsesquioxanes on the miscibility and specific interaction with phenolic blends. *Macromolecules* **2006**, *39*, 300−308.
(16) Lin, H. C.; Kuo, S. W.; Huang, C. F.; Chang, F. C. Thermal and surface properties of phenolic nanocomposites containing octaphenol polyhedral oligomeric silsesquioxane. *Macromol. Rapid Commun.* **2006**, *27*, 537−541.
(17) Lee, Y. J.; Huang, J. M.; Kuo, S. W.; Lu, J. S.; Chang, F. C. Polyimide and polyhedral oligomeric silsesquioxane nanocomposites for low-dielectric applications. *Polymer* **2005**, *46*, 173−181.
(18) Pan, Q. W.; Smith, D. M.; Qi, H.; Wang, S. J.; Li, C. Y. Highly Efficient Hybrid Electrolytes with Controlled Network Structures for Lithium-metal Batteries. *Adv. Mater.* **2015**, *27*, 5995−6001.
(19) Han, S. Y.; Wang, X. M.; Shao, Y.; Guo, Q. Y.; Li, Y.; Zhang, W. B. Janus POSS Based on Mixed [2:6] Octakis-Adduct Regioisomers. *Chem. - Eur. J.* **2016**, *22*, 6397−6403.
(20) Wang, X. M.; Shao, Y.; Xu, J.; Jin, X.; Shen, R. H.; Jin, P. F.; Shen, D. W.; Wang, J.; Li, W.; He, J.; Ni, P.; Zhang, W. B. Precision Synthesis and Distinct Assembly of Double-chain Giant Surfactant Regio-isomers. *Macromolecules* **2017**, *50*, 3943.
(21) Wu, S.; Hayakawa, T.; Kikuchi, R.; Grunzinger, S. J.; Kakimoto, M.; Oikawa, H. Synthesis and characterization of semiaromatic polyimides containing POSS in main chain derived from double-decker-shaped silsesquioxane. *Macromolecules* **2007**, *40*, 5698−5705.
(22) Wu, S.; Hayakawa, T.; Kakimoto, M.; Oikawa, H. Synthesis and Characterization of Organosoluble Aromatic Polyimides Containing POSS in Main Chain Derived from Double-Decker-Shaped Silsesquioxane. *Macromolecules* **2008**, *41*, 3481−3487.
(23) Wei, K.; Wang, L.; Zheng, S. Organic−inorganic polyurethanes with 3,13-dihydroxypropyloctaphenyl double-decker silsesquioxane chain extender. *Polym. Chem.* **2013**, *4*, 1491−1501.
(24) Liu, N.; Li, L.; Wang, L.; Zheng, S. Organic-inorganic polybenzoxazine copolymers with double decker silsesquioxanes in the main chains: Synthesis and thermally activated ring-opening polymerization behavior. *Polymer* **2017**, *109*, 254−265.
(25) Ishida, H. In *Handbook of Benzoxazine Resins*; Ishida, H., Agag, T., Eds.; Elsevier: Amsterdam, 2011; Chapter 1, pp 3−81.
(26) Ghosh, N. N.; Kiskan, B.; Yagci, Y. Polybenzoxazines - New high performance thermosetting resins: Synthesis and properties. *Prog. Polym. Sci.* **2007**, *32*, 1344−1391.
(27) Ohashi, S.; Kilbane, J.; Heyl, T.; Ishida, H. Synthesis and characterization of cyanate ester functional benzoxazine and its polymer. *Macromolecules* **2015**, *48*, 8412−8417.
(28) Zhang, K.; Liu, J.; Ishida, H. An ultrahigh performance cross-linked polybenzoxazole via thermal conversion from poly(benzoxazine amic acid) based on smart o-benzoxazine chemistry. *Macromolecules* **2014**, *47*, 8674−8681.
(29) Lin, R. C.; Mohamed, M. G.; Hsu, K. C.; Wu, J. Y.; Jheng, Y. R.; Kuo, S. W. Multivalent photo-crosslinkable coumarin-containing polybenzoxazines exhibiting enhanced thermal and hydrophobic surface properties. *RSC Adv.* **2016**, *6*, 10683−10696.
(30) Wang, C. F.; Su, Y. C.; Kuo, S. W.; Huang, C. F.; Sheen, Y. C.; Chang, F. C. Low-surface-free-energy materials based on polybenzoxazines. *Angew. Chem., Int. Ed.* **2006**, *45*, 2248−2251.
(31) Ye, Y. S.; Huang, Y. J.; Chang, F. C.; Xue, Z. G.; Xie, X. L. Synthesis and characterization of thermally cured polytriazole polymers incorporating main or side chain benzoxazine crosslinking moieties. *Polym. Chem.* **2014**, *5*, 2863−2871.
(32) Qu, L.; Xin, Z. Preparation and surface properties of novel low surface free energy fluorinated silane-functional polybenzoxazine films. *Langmuir* **2011**, *27*, 8365−8370.
(33) Zhang, K.; Zhuang, Q.; Zhou, Y.; Liu, X.; Yang, G.; Han, Z. Preparation and properties of novel low dielectric constant benzoxazole-based polybenzoxazine. *J. Polym. Sci., Part A: Polym. Chem.* **2012**, *50*, 5115−5123.
(34) Kudoh, R.; Sudo, A.; Endo, T. A highly reactive benzoxazine monomer, 1-(2-hydroxyethyl)-1,3-benzoxazine: Activation of benzoxazine by neighboring group participation of hydroxyl group. *Macromolecules* **2010**, *43*, 1185−1187.
(35) Velez-Herrera, P.; Doyama, K.; Abe, H.; Ishida, H. Synthesis and characterization of highly fluorinated polymer with the benzoxazine moiety in the main chain. *Macromolecules* **2008**, *41*, 9704−9714.
(36) Hu, H. W.; Huang, K. W.; Kuo, S. W. Heteronucleobase-functionalized benzoxazine: synthesis, thermal properties, and self-assembled structure formed through multiple hydrogen bonding interactions. *Polym. Chem.* **2012**, *3*, 1546−1554.
(37) Yang, C. C.; Lin, Y. C.; Wang, P. I.; Liaw, D. J.; Kuo, S. W. Polybenzoxazine/single-walled carbon nanotube nanocomposites stabilized through noncovalent bonding interactions. *Polymer* **2014**, *55*, 2044−2050.
(38) Fu, H. K.; Huang, C. F.; Kuo, S. W.; Lin, H. C.; Yei, D. R.; Chang, F. C. Effect of an organically modified nanoclay on low-

DOI: 10.1021/acs.macromol.7b01085
Macromolecules 2017, 50, 5739−5747

surface-energy materials of polybenzoxazine. *Macromol. Rapid Commun.* **2008**, *29*, 1216−1220.
(39) Mohamed, M. G.; Kuo, S. W. Polybenzoxazine/polyhedral oligomeric silsesquioxane (POSS) nanocomposites. *Polymers* **2016**, *8*, 225.
(40) Cui, H. W.; Kuo, S. W. Nanocomposites of polybenzoxazine and exfoliated montmorillonite using a polyhedral oligomeric silsesquioxane surfactant and click chemistry. *J. Polym. Res.* **2013**, *20*, 1−13.
(41) Meng, F. B.; Ishida, H.; Liu, X. B. Introduction of benzoxazine onto the graphene oxide surface by click chemistry and the properties of graphene oxide reinforced polybenzoxazine nanohybrids. *RSC Adv.* **2014**, *4*, 9471−9475.
(42) Shih, H. K.; Hsieh, C. C.; Mohamed, G. M.; Zhu, C. Y.; Kuo, S. W. Ternary polybenzoxazine/POSS/SWCNT hybrid nanocomposites stabilized through supramolecular interactions. *Soft Matter* **2016**, *12*, 1847−1858.
(43) Su, W. C.; Kuo, S. W. Reversible surface properties of polybenzoxazine/silica nanocomposites thin films. *J. Nanomater.* **2013**, *2013*, 1−12.
(44) Huang, K. W.; Kuo, S. W. High Performance Polybenzoxazine Nanocomposites Containing Multifunctional POSS Cores Presenting Vinyl-Terminated Benzoxazine Groups. *Macromol. Chem. Phys.* **2010**, *211*, 2301−2311.

DOI: 10.1021/acs.macromol.7b01085
Macromolecules 2017, 50, 5739−5747